Supporting Information for Pariser-Parr-Pople Model based Investigation of Ground and Low-Lying Excited States of Long Acenes

Himanshu Chakraborty and Alok Shukla*

Department of Physics, Indian Institute of Technology Bombay, Powai, Mumbai 400076, INDIA

E-mail: chakraborty.himanshu@gmail.com,shukla@phy.iitb.ac.in

*To whom correspondence should be addressed

Convergence of Excitation Energies in MRSDCI Calculations

Figure 1: Behavior of 1^1B_{2u} (circles), 1^3B_{2u} (squares) excited states of nonacene with respect to the number of reference configurations (N_{ref}) included in the MRSDCI calcualtions performed using the screened parameters.

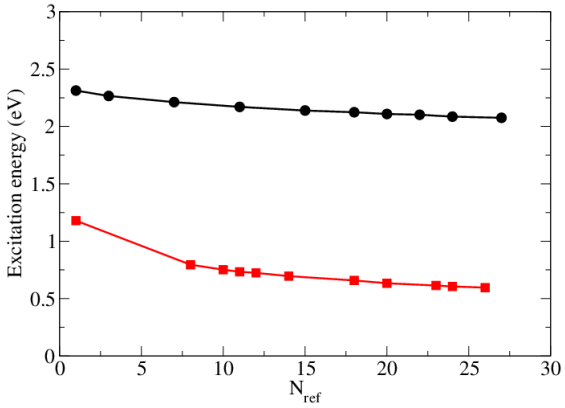

In order to demonstate the convergence of our MRSDCI calculations, we present the plot of the excitation energies of two lowest states, singlet $1^1B_{2u}^+$ and triplet $1^3B_{2u}^+$, of nonacene, computed using the screened parameters, in Figure 1, calculated with increasing number of reference configurations (N_{ref}). It is obvious from the figure that the convergence has been achieved by the time twenty most important configurations ($N_{ref} = 20$) have been included in the calculations.

Influence of the Geometry on the Optical Absorption in Long Acenes

The issue of the ground state geometry in long acenes has been in debate for many years.[1–5] Some theoretical calculations have predicted a symmetric ground state geometry to be lower,[1,2] while others have indicated a highly non-uniform geometry to be the true ground state.[3–5] In this work, consistent with the PPP model based work of Ramasesha and cowork-

ers,[1,2] and our own work,[6,7] we have used the symmetric ground state geometry for all oligoacenes, with all the C-C bonds equal to 1.4 Å, and all bond angles taken to be 120^o. In order to investigate the influence of geometry on the optical absorption spectra, we performed calculations on nonacene using a highly non-uniform geometry reported for its closed-shell singlet ground state by Bendikov *et al.*,[3] obtained using the B3LYP exchange-correlation functional in DFT. As compared to the symmetric geometry, the nonuniformity is quite severe in this geometry, with the two polyene chains exhibiting bond alternation, and the inter-chain separation also varying significantly. The smallest C-C bond length in the nonuniform structure is ≈ 1.36 Å, while the largest one is close to 1.47 Å. For this nonuniform geometry, the hopping matrix elements between nearest-neighbor sites i and j, needed for the PPP calculations, were generated using the exponential formula $t_{ij} = t_0 e^{(r_0 - r_{ij})/\delta}$, where r_{ij} is the bond distance (in Å) between the sites, $t_0 = -2.4$ eV, $r_0 = 1.4$ Å, and the decay constant $\delta = 0.73$ Å. The value of δ was chosen so that the formula closely reproduces the hopping matrix elements for a bond-alternating polyene with short/long bonds 1.35/1.45 Å. The results of an SCI level calculation of the singlet optical absorption spectrum of nonacene, both for the uniform (symmetric) and this nonuniform geometry of Bendikov *et al.*,[3] computed using the screened parameters of the PPP model, are presented in Figure. 2. From the figure it is obvious that there are small quantitative differences between the two results, as far as peak locations are concerned. For example, the first peak (1^1B_{2u}) is slightly blueshifted (0.11 eV) for the nonuniform geometry, as compared to the symmetric geometry, while the most intense peak (1^1B_{3u}) is slightly redshifted (0.15 eV). The only qualitative change between the two results is at an energy higher than 5.5 eV, where one peak in the nonuniform geometry is more intense as compared to its neighboring peak. Therefore, we conclude that the variations in the ground state geometries of the magnitude considered here, lead to small quantitative, and insignificant qualitative, changes in the optical absorption spectra of oligoacenes.

Figure 2: Comparison of the calculated singlet optical absorption spectra for nonacene, with the uniform (symmetric) geometry, and the nonuniform geometry of Bendikov *et al.*,[3] computed at SCI level, employing the screened parameters in the PPP model.

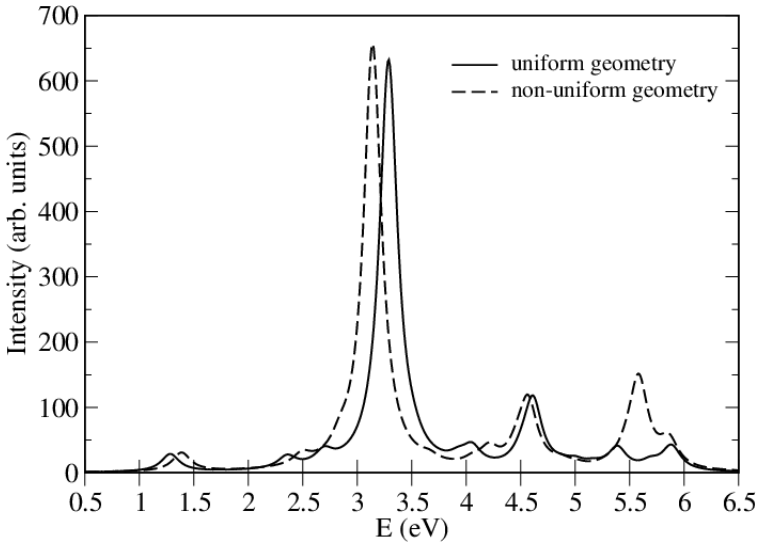

Singlet linear absorption

In the following, we discuss in detail the calculated singlet linear absorption spectra of octacene, nonacene, and decacene, presented in Figures 4–6 of the main text for the standard and the screened parameters. Furthermore, Tables 1–6, provide exhaustive information about the excited states contributing to the singlet absorption spectra of these oligomers.

1. For all the oligoacene, the first peak is due to a y-polarized transition, to the $1^1B^+_{2u}$ excited state of the system, whose wave function is dominated by the $|H \rightarrow L\rangle$ single excitation, irrespective of the choice of the Coulomb parameters employed in the PPP model.

2. The second peak also corresponds to a y-polarized transition, to the $2^1B^+_{2u}$ excited state of the system. The most important configuration contributing to the many-particle wave function of this state is $|H-1 \rightarrow L+1\rangle$ excitation, irrespective of the choice of

the Coulomb parameters.

3. The nature of the third peak is dependent upon the Coulomb parameters employed in the PPP model. For the standard parameter case, this peak always corresponds to the x-polarized, $1^1B^+_{3u}$ excited state, signalling the onset of the most intense absorption feature in the system. For octacene, it is the single most intense peak, whose wave function mainly consists of single excitations $|H \rightarrow L+3\rangle + c.c.$ ($c.c.$ denotes the charge conjugated configuration). For nonacene and decacene, perhaps due to band formation, it is the first of the two adjacent intense peaks which are x polarized. For nonacene it is the most intense peak, and the corresponding many-body wave function is dominated by the single excitation $|H \rightarrow L+4\rangle + c.c.$. For decacene, however, it is the second most intense feature, and the double excitations $|H \rightarrow L;\ H \rightarrow L+1\rangle + c.c.$ contribute the most to its many-body wave function.

   In the screened parameter calculations, the third peak is a faint peak, containing a mixture of x and y polarized transition to the states, $1^1B^+_{3u}$ and $3^1B^+_{2u}$ of the system. For all the oligoacenes, the double excitation $|H \rightarrow L;\ H \rightarrow L+1\rangle + c.c.$ contributes the most to the $1^1B^+_{3u}$ state, and the single excitation $|H \rightarrow L+2\rangle + c.c.$ dominates the $3^1B^+_{2u}$ wave function.

4. For the standard parameter case, the fourth peak is a faint peak for octacene, consisting of a mixture of x- and y-polarized transitions to the states, $2^1B^+_{3u}$ and $4^1B^+_{2u}$. Double excitations $|H \rightarrow L;\ H \rightarrow L+1\rangle + c.c.$ contribute the most to the $2^1B^+_{3u}$ state, and single excitations $|H-2 \rightarrow L+2\rangle + c.c.$ to the $4^1B^+_{2u}$ state. For nonacene and decacene, however, it is an intense x-polarized feature corresponding to the state $2^1B^+_{3u}$, which is adjacent to their $1^1B^+_{3u}$ state mentioned above. For the case of decacene, it also the most intense absorption of the system. Both for nonacene and decacene, the single excitations $|H \rightarrow L+4\rangle + c.c.$ contribute the most to the many-particle wave

function of this state.

For the screened parameter calculations, the fourth peak corresponds to the most intense absorption, through an x-polarized photon, to the $2^1B^+_{3u}$ state, in case of octacene and nonacene. For decacene, however, it appears as a shoulder to the most intense peak, consisting of a mixture of x and y polarized transitions, to the $2^1B^+_{3u}$ and $4^1B^+_{2u}$ states. The many-particle wave function of the $2^1B^+_{3u}$ state for octacene and nonacene is dominated by the single excitations $|H \rightarrow L+4\rangle + c.c.$, while for decacene the double excitations $|H \rightarrow L+1;\ H \rightarrow L+2\rangle + c.c.$ dominate. The $4^1B^+_{2u}$ state of decacene has the maximum contribution from the single excitation $|H-2 \rightarrow L+2\rangle$.

5. For the standard parameter case, the fifth peak is a very faint feature consisting of y-polarized transition to the state $7^1B^+_{2u}$ for octacene, whose wave function is dominated by the single excitation $|H-2 \rightarrow L+2\rangle$. However, for nonacene and decacene, it corresponds to the mixture of x and y polarized transitions to the states, $3^1B^+_{3u}$ and $5^1B^+_{2u}$, respectively. The double excitations $|H \rightarrow L+1;\ H-1 \rightarrow L+1\rangle + c.c.$ for the $3^1B^+_{3u}$ state, and the triple excitation $|H \rightarrow L;\ H \rightarrow L;\ H-1 \rightarrow L+1\rangle$ for the $5^1B^+_{2u}$ state, contribute the most to their wave functions.

   For the screened parameter case, it is a faint peak consisting of a mixture of x and y polarized transitions to the states, $3^1B^+_{3u}$ and $4^1B^+_{2u}$, respectively, for both octacene and nonacene. For decacene, however, it is the most intense peak corresponding to x polarized transition to the state $4^1B^+_{3u}$. The most important configuration contributing to the many-particle wave function of the state for octacene and nonacene, is a mixture of double excitations $|H \rightarrow L+1;\ H \rightarrow L+2\rangle + c.c.$ for $3^1B^+_{3u}$ state, and single excitations $|H-2 \rightarrow L+2\rangle$ for the $4^1B^+_{2u}$ state. For decacene, the single excitations $|H \rightarrow L+5\rangle + c.c.$ contribute the most to the wavefunction of this state.

6. For the standard parameter case, the sixth peak corresponds to a mixture of x and y polarized transitions to the states, $4^1B^+_{3u}$ and $9^1B^+_{2u}$, respectively, for octacene. The many-body wave functions of both these states derive predominant contributions from double excitations: $|H \rightarrow L;\, H-1 \rightarrow L+2\rangle + c.c.$ for the $4^1B^+_{3u}$, and $|H \rightarrow L+1;\, H \rightarrow L+3\rangle + c.c.$ for the $9^1B^+_{2u}$ state. For nonacene (decacene), it corresponds to a y-polarized transition to the state $10^1B^+_{2u}$ ($9^1B^+_{2u}$), whose many-body wave function derives maximum contribution from the single excitation $|H-2 \rightarrow L+2\rangle$.

   The same peak with the screened parameters is a mixture of x and y polarized transitions for the case of octacene and nonacene. For octacene, transitions to states $6^1B^+_{3u}$ and $8^1B^+_{2u}$ constitute this peak, with double excitations $|H \rightarrow L;\, H \rightarrow L+1\rangle + c.c.$ and $|H \rightarrow L;\, H \rightarrow L+5\rangle + c.c.$, respectively, contributing most to their wave functions. For nonacene, this peak consists of three states $4^1B^+_{3u}$ and $6^1B^+_{2u}$ and $7^1B^+_{2u}$, with double excitation $|H \rightarrow L;\, H-1 \rightarrow L+2\rangle + c.c.$ contributing the most to the $4^1B^+_{3u}$, triple excitation $|H \rightarrow L;\, H \rightarrow L;\, H-1 \rightarrow L+1\rangle$ to the $6^1B^+_{2u}$, and the single excitation $|H-2 \rightarrow L+2\rangle$ to the $7^1B^+_{2u}$ state. However, for decacene, the peak is purely x polarized, due to transition to the state $6^1B^+_{3u}$ whose wave function derives maximum contribution from the double excitations $|H \rightarrow L;\, H \rightarrow L+1\rangle + c.c.$.

7. The seventh peak in the standard parameter spectrum is both x and y polarized for all the three oligomers. For octacene, the peak involves $5^1B^+_{3u}$ and $10^1B^+_{2u}$ states, with single excitations $|H \rightarrow L+7\rangle + c.c.$ and $|H-2 \rightarrow L+2\rangle$, respectively, contributing the most to their wave functions. For nonacene states $7^1B^+_{3u}$ and $12^1B^+_{2u}$ constitute the peak, with single excitation $|H \rightarrow L+8\rangle$+c.c. providing the maximum contribution to the $7^1B^+_{3u}$ state, and triple excitation $|H \rightarrow L;\, H-1 \rightarrow L+1;\, H-1 \rightarrow L+1\rangle$ to the $12^1B^+_{2u}$ state. For decacene, the peak involves $6^1B^+_{3u}$ and $11^1B^+_{2u}$ states, with double excitations $|H \rightarrow L;\, H-1 \rightarrow L+2\rangle + c.c.$ and triple excitations $|H \rightarrow L;\, H-1 \rightarrow L+1;\, H-1 \rightarrow L+1\rangle$, respectively, contributing the most to their wave functions.

With the screened parameters, the seventh peak of octacene and nonacene is x polarized, while for decacene it has mixed x and y polarizations. Both for octacene and nonacene states $8^1B^+_{3u}$ constitute this peak, with single excitation $|H-1 \rightarrow L+5\rangle + c.c.$ and $|H-1 \rightarrow L+6\rangle + c.c.$ providing main contributions to the wave functions of octacene, and nonacene, respectively. However, for decacene, transitions to states $8^1B^+_{3u}$ and $10^1B^+_{2u}$ form the peak, with double excitations $|H \rightarrow L;\ H-1 \rightarrow L+4\rangle + c.c.$ and single excitations $|H-1 \rightarrow L+7\rangle + c.c.$, respectively, contributing the most to their wave functions.

8. With the standard parameters, the eighth peak does not exist for octacene, while for nonacene and decacene, it has mixed x and y polarizations. For nonacene, the states constituting the peak are $8^1B^+_{3u}$ and $16^1B^+_{2u}$, with single excitations $|H-1 \rightarrow L+5\rangle + c.c.$ and triple excitations $|H \rightarrow L;\ H \rightarrow L+2;\ H-1 \rightarrow L+1\rangle + c.c.$, respectively, contributing to their wave functions. For decacene, three states $7^1B^+_{3u}$, $14^1B^+_{2u}$, and $15^1B^+_{2u}$, form this peak, with single excitations $|H \rightarrow L+8\rangle + c.c.$, $|H \rightarrow L+12\rangle + c.c.$, and $|H \rightarrow L+9\rangle + c.c.$, respectively, contributing the most to their many-particle wave functions.

   With the screened parameters case, the eighth peak is x and y polarized for octacene and decacene, while it is only x polarized for nonacene. For octacene, states $9^1B^+_{3u}$ and $13^1B^+_{2u}$ form this peak, whose wave functions, respectively, derive maximum contributions from single excitations $|H-2 \rightarrow L+4\rangle + c.c.$, and triple excitations $|H \rightarrow L;\ H-1 \rightarrow L+1;\ H-1 \rightarrow L+1\rangle$. In case of nonacene, the transition to the state $9^1B^+_{3u}$ leads to this peak, with single excitations $|H-2 \rightarrow L+4\rangle + c.c.$ contributing the most to its many-particle wave function. For decacene, states $9^1B^+_{3u}$ and $14^1B^+_{2u}$ constitute the peak, with the single excitations $|H \rightarrow L+8\rangle + c.c.$ and $|H \rightarrow L+9\rangle + c.c.$, respectively, providing the largest contributions to their wave

functions.

9. The ninth peak, for the standard parameter case, exists only for decacene, and has a mixed x and y polarization, with states $8^1B_{3u}^+$ and $17^1B_{2u}^+$ forming the peak. The single excitations $|H-2 \rightarrow L+4\rangle + c.c.$ contribute the most to $8^1B_{3u}^+$ state, while double excitations $|H \rightarrow L;\ H-1 \rightarrow L+4\rangle + c.c.$ to the $17^1B_{2u}^+$ state.

   With the screened parameters, the ninth peak does not exist for nonacene, and it is x and y polarized for octacene and decacene. For octacene, states $12^1B_{3u}^+$ and $16^1B_{2u}^+$ constitute this peak, with the double excitations $|H \rightarrow L;\ H-1 \rightarrow L+6\rangle + c.c.$ and single excitations $|H-1 \rightarrow L+7\rangle + c.c.$, respectively, contributing the most to their wave functions. For decacene, the states $11^1B_{3u}^+$ and $16^1B_{2u}^+$ form this peak, with the single excitations $|H-2 \rightarrow L+5\rangle + c.c.$ and $|H-1 \rightarrow L+7\rangle + c.c.$, respectively, providing the maximum contributions to their wave functions.

Table 1: Excited states contributing to the singlet linear absorption spectrum of octacene computed using the MRSDCI method coupled with the standard parameters in the PPP model Hamiltonian. The table includes many-particle dominant contributing configurations, excitation energies, dipole matrix elements, and relative oscillator strengths (ROS) of various states with respect to the 1^1A_g ground state. DF corresponds to dipole forbidden state. Below, '$+c.c.$' indicates that the coefficient of charge conjugate of a given configuration has the same sign, while '$-c.c.$' implies that the two coefficients have opposite signs.

Peak	State	E (eV)	Transition	ROS	dominant contributing configurations
			Dipole (Å)		
DF	$1^1B_{3u}^-$	2.31	0	0	$\|H \to L; H \to L+1\rangle - c.c.(0.4948)$
					$\|H \to L; H-1 \to L+2\rangle - c.c.(0.1938)$
I	$1^1B_{2u}^+$	2.24	0.905	0.034	$\|H \to L\rangle\ (-0.8471)$
					$\|H \to L; H \to L; H-1 \to L+1\rangle\ (0.0948)$
II	$2^1B_{2u}^+$	3.34	0.641	0.025	$\|H-1 \to L+1\rangle\ (-0.5826)$
					$\|H \to L+2\rangle - c.c.(0.4284)$
III	$1^1B_{3u}^+$	4.17	3.622	1.000	$\|H \to L+3\rangle + c.c.(0.4622)$
					$\|H \to L; H \to L+1\rangle + c.c.(0.2614)$
IV	$4^1B_{2u}^+$	4.51	0.367	0.011	$\|H-2 \to L+2\rangle\ (-0.4148)$
					$\|H-1 \to L+4\rangle + c.c.(0.4020)$
	$2^1B_{3u}^+$	4.57	1.079	0.097	$\|H \to L; H \to L+1\rangle + c.c.(0.3214)$
					$\|H \to L+3\rangle + c.c.(0.3214)$
V	$7^1B_{2u}^+$	5.46	0.375	0.014	$\|H-2 \to L+2\rangle\ (0.3574)$
					$\|H \to L+6\rangle - c.c.(0.3489)$
VI	$9^1B_{2u}^+$	5.64	0.261	0.007	$\|H \to L+1; H \to L+3\rangle + c.c.(0.3883)$
					$\|H \to L; H \to L+5\rangle + c.c.(0.2768)$
	$4^1B_{3u}^+$	5.65	0.335	0.012	$\|H \to L; H-1 \to L+2\rangle - c.c.(0.4696)$
					$\|H \to L; H \to L+1\rangle + c.c.(0.1289)$
VII	$10^1B_{2u}^+$	5.89	0.203	0.004	$\|H-2 \to L+2\rangle\ (-0.3657)$
					$\|H-3 \to L+3\rangle\ (0.3074)$
	$5^1B_{3u}^+$	5.94	0.307	0.010	$\|H \to L+7\rangle - c.c.(0.3397)$
					$\|H \to L; H \to L+4\rangle + c.c.(0.2494)$

Table 2: Excited states contributing to the singlet linear absorption spectrum of octacene computed using the MRSDCI method coupled with the screened parameters in the PPP model Hamiltonian. The rest of the information is same as that in Table 1.

Peak	State	E (eV)	Transition Dipole (Å)	ROS	dominant contributing configurations
DF	$1^1B_{3u}^-$	1.59	0	0	$\|H \rightarrow L; H \rightarrow L+1\rangle - c.c.(0.5078)$
					$\|H \rightarrow L; H-1 \rightarrow L+2\rangle - c.c.(0.1949)$
I	$1^1B_{2u}^+$	1.49	1.241	0.050	$\|H \rightarrow L\rangle$ (0.8503)
					$\|H \rightarrow L; H \rightarrow L; H-1 \rightarrow L+1\rangle$ (0.0929)
II	$2^1B_{2u}^+$	2.65	0.897	0.047	$\|H-1 \rightarrow L+1\rangle$ (−0.7244)
					$\|H \rightarrow L+2\rangle + c.c.(0.2638)$
III	$3^1B_{2u}^+$	2.89	0.440	0.012	$\|H \rightarrow L+2\rangle + c.c.(0.5326)$
					$\|H-1 \rightarrow L+1\rangle$ (−0.3290)
	$1^1B_{3u}^+$	2.97	0.845	0.046	$\|H \rightarrow L; H \rightarrow L+1\rangle - c.c.(0.4942)$
					$\|H \rightarrow L+1; H-1 \rightarrow L+1\rangle - c.c.(0.2522)$
IV	$2^1B_{3u}^+$	3.38	3.675	1.000	$\|H \rightarrow L+4\rangle + c.c.(0.5831)$
					$\|H-1 \rightarrow L+5\rangle + c.c.(0.1004)$
V	$3^1B_{3u}^+$	3.91	0.410	0.014	$\|H \rightarrow L+1; H \rightarrow L+2\rangle - c.c.(0.4028)$
					$\|H \rightarrow L+1; H \rightarrow L+4\rangle - c.c.(0.3003)$
	$4^1B_{2u}^+$	3.97	0.641	0.036	$\|H-2 \rightarrow L+2\rangle$ (−0.5280)
					$\|H-1 \rightarrow L+3\rangle + c.c.(0.3722)$
VI	$8^1B_{2u}^+$	4.52	0.230	0.005	$\|H \rightarrow L; H \rightarrow L+5\rangle - c.c.(0.4706)$
					$\|H \rightarrow L; H-1 \rightarrow L+4\rangle - c.c.(0.3075)$
	$6^1B_{3u}^+$	4.57	0.403	0.016	$\|H \rightarrow L; H \rightarrow L+1\rangle - c.c.(0.3419)$
					$\|H \rightarrow L; H \rightarrow L+3\rangle - c.c.(0.2890)$
VII	$8^1B_{3u}^+$	4.80	1.301	0.178	$\|H-1 \rightarrow L+5\rangle + c.c.(0.5537)$
					$\|H \rightarrow L; H-1 \rightarrow L+2\rangle - c.c.(0.1321)$
VIII	$9^1B_{3u}^+$	5.14	0.410	0.019	$\|H-2 \rightarrow L+4\rangle + c.c.(0.5720)$
					$\|H \rightarrow L+2; H \rightarrow L+3\rangle - c.c.(0.0943)$
	$13^1B_{2u}^+$	5.22	0.418	0.020	$\|H \rightarrow L; H-1 \rightarrow L+1; H-1 \rightarrow L+1\rangle$ (0.3505)
					$\|H-1 \rightarrow L+7\rangle + c.c.(0.2709)$
IX	$16^1B_{2u}^+$	5.53	0.440	0.023	$\|H-1 \rightarrow L+7\rangle + c.c.(0.3983)$
					$\|H-3 \rightarrow L+3\rangle$ (0.3636)
	$12^1B_{3u}^+$	5.66	0.154	0.003	$\|H \rightarrow L; H-1 \rightarrow L+6\rangle - c.c.(0.4014)$
					$\|H \rightarrow L+2; H-2 \rightarrow L+1\rangle - c.c.(0.3019)$

Table 3: Excited states contributing to the singlet linear absorption spectrum of nonacene computed using the MRSDCI method coupled with the standard parameters in the PPP model Hamiltonian. The rest of the information is same as that in Table 1.

Peak	State	E (eV)	Transition Dipole (Å)	ROS	dominant contributing configurations
DF	$1^1B^-_{3u}$	1.86	0	0	$\|H \to L; H \to L+1\rangle + c.c.(0.4872)$
					$\|H \to L+1; H \to L+2\rangle + c.c.(0.2027)$
I	$1^1B^+_{2u}$	1.82	1.328	0.092	$\|H \to L\rangle$ (0.8290)
					$\|H \to L; H \to L; H-1 \to L+1\rangle$ (0.1066)
II	$2^1B^+_{2u}$	2.79	0.733	0.043	$\|H-1 \to L+1\rangle$ (0.5506)
					$\|H \to L+2\rangle + c.c.(0.4342)$
III	$1^1B^+_{3u}$	3.80	3.037	1.000	$\|H \to L+4\rangle - c.c.(0.3757)$
					$\|H \to L; H \to L+1\rangle - c.c.(0.3274)$
IV	$2^1B^+_{3u}$	4.12	2.583	0.786	$\|H \to L+4\rangle - c.c.(0.3943)$
					$\|H \to L; H \to L+1\rangle - c.c.(0.2791)$
V	$5^1B^+_{2u}$	4.62	0.439	0.025	$\|H \to L; H \to L; H-1 \to L+1\rangle$ (0.6215)
					$\|H-1 \to L+1\rangle$ (0.2357)
	$3^1B^+_{3u}$	4.63	0.549	0.040	$\|H \to L+1; H-1 \to L+1\rangle - c.c.(0.3339)$
					$\|H \to L+1; H \to L+2\rangle - c.c.(0.3035)$
VI	$10^1B^+_{2u}$	5.29	0.457	0.032	$\|H-2 \to L+2\rangle$ (−0.3824)
					$\|H \to L+1; H \to L+4\rangle + c.c.(0.2681)$
VII	$7^1B^+_{3u}$	5.71	0.277	0.013	$\|H \to L+8\rangle - c.c.(0.3021)$
					$\|H \to L; H \to L+3\rangle + c.c.(0.2619)$
	$12^1B^+_{2u}$	5.72	0.318	0.017	$\|H \to L; H-1 \to L+1; H-1 \to L+1\rangle$ (−0.3293)
					$\|H \to L; H-1 \to L+4\rangle - c.c.(0.2869)$
VIII	$16^1B^+_{2u}$	5.94	0.287	0.014	$\|H \to L; H \to L+2; H-1 \to L+1\rangle - c.c.(0.3742)$
					$\|H \to L; H-1 \to L+4\rangle - c.c.(0.2500)$
	$8^1B^+_{3u}$	5.95	0.996	0.169	$\|H-1 \to L+5\rangle - c.c.(0.3932)$
					$\|H-2 \to L+4\rangle - c.c.(0.2993)$

Table 4: Excited states contributing to the singlet linear absorption spectrum of nonacene computed using the MRSDCI method coupled with the screened parameters in the PPP model Hamiltonian. The rest of the information is same as that in Table 1.

Peak	State	E (eV)	Transition Dipole (Å)	ROS	dominant contributing configurations
DF	$1^1B^-_{3u}$	1.51	0	0	$\|H \to L; H \to L+1\rangle + c.c.(0.5143)$
					$\|H \to L; H-1 \to L+2\rangle - c.c.(0.2089)$
I	$1^1B^+_{2u}$	1.46	1.316	0.051	$\|H \to L\rangle\ (0.8551)$
					$\|H \to L; H \to L; H-1 \to L+1\rangle\ (0.1017)$
II	$2^1B^+_{2u}$	2.45	0.935	0.043	$\|H-1 \to L+1\rangle\ (0.7260)$
					$\|H \to L+2\rangle - c.c.(0.2689)$
III	$1^1B^+_{3u}$	2.71	0.611	0.020	$\|H \to L; H \to L+1\rangle - c.c.(0.4901)$
					$\|H \to L+1; H-1 \to L+1\rangle - c.c.(0.2454)$
	$3^1B^+_{2u}$	2.77	0.507	0.014	$\|H \to L+2\rangle - c.c.(0.5434)$
					$\|H-1 \to L+1\rangle\ (-0.3462)$
IV	$2^1B^+_{3u}$	3.32	3.887	1.000	$\|H \to L+4\rangle - c.c.(0.5689)$
					$\|H-1 \to L+6\rangle + c.c.(0.1185)$
V	$3^1B^+_{3u}$	3.63	0.782	0.044	$\|H \to L+1; H \to L+2\rangle + c.c.(0.3441)$
					$\|H-1 \to L+1; H \to L+1\rangle - c.c.(0.3221)$
	$4^1B^+_{2u}$	3.69	0.559	0.023	$\|H-2 \to L+2\rangle\ (-0.4715)$
					$\|H-1 \to L+3\rangle + c.c.(0.4395)$
VI	$4^1B^+_{3u}$	3.93	0.369	0.011	$\|H \to L; H-1 \to L+2\rangle - c.c.(0.4953)$
					$\|H \to L; H \to L+3\rangle - c.c.(0.2163)$
	$6^1B^+_{2u}$	4.01	0.690	0.038	$\|H \to L; H \to L; H-1 \to L+1\rangle\ (0.5954)$
					$\|H \to L+5\rangle + c.c.(0.3166)$
	$7^1B^+_{2u}$	4.12	0.692	0.039	$\|H-2 \to L+2\rangle\ (-0.5949)$
					$\|H-1 \to L+3\rangle + c.c.(0.3994)$
VII	$8^1B^+_{3u}$	4.61	1.450	0.193	$\|H-1 \to L+6\rangle + c.c.(0.5262)$
					$\|H \to L; H-1 \to L+2\rangle - c.c.(0.1473)$
VIII	$9^1B^+_{3u}$	4.97	0.338	0.011	$\|H-2 \to L+4\rangle + c.c.(0.5823)$
					$\|H \to L+8\rangle + c.c.(0.0699)$

Table 5: Excited states contributing to the singlet linear absorption spectrum of decacene computed using the MRSDCI method coupled with the standard parameters in the PPP model Hamiltonian. The rest of the information is same as that in Table 1.

Peak	State	E (eV)	Transition Dipole (Å)	ROS	dominant contributing configurations
DF	$1^1B^-_{3u}$	1.72	0	0	$\|H \to L; H \to L+1\rangle - c.c.(0.4790)$
					$\|H \to L+1; H \to L+2\rangle + c.c.(0.2119)$
I	$1^1B^+_{2u}$	1.79	1.423	0.084	$\|H \to L\rangle\ (-0.8203)$
					$\|H-1 \to L+1\rangle\ (-0.1213)$
II	$2^1B^+_{2u}$	2.64	0.776	0.037	$\|H-1 \to L+1\rangle\ (-0.5607)$
					$\|H \to L+2\rangle - c.c.(0.4239)$
III	$1^1B^+_{3u}$	3.68	2.554	0.553	$\|H \to L; H \to L+1\rangle + c.c.(0.3710)$
					$\|H \to L+4\rangle + c.c.(0.2865)$
IV	$2^1B^+_{3u}$	4.00	3.293	1.000	$\|H \to L+4\rangle + c.c.(0.4451)$
					$\|H \to L+1; H \to L+2\rangle - c.c.(0.2322)$
V	$5^1B^+_{2u}$	4.40	0.505	0.026	$\|H \to L; H \to L; H-1 \to L+1\rangle\ (-0.6203)$
					$\|H-1 \to L+1\rangle\ (-0.2380)$
	$3^1B^+_{3u}$	4.46	0.739	0.056	$\|H \to L+1; H-1 \to L+1\rangle + c.c.(0.3459)$
					$\|H \to L+1; H \to L+2\rangle - c.c.(0.2800)$
VI	$9^1B^+_{2u}$	5.05	0.392	0.018	$\|H-2 \to L+2\rangle\ (-0.3901)$
					$\|H-1 \to L+3\rangle\ (-0.2482)$
VII	$6^1B^+_{3u}$	5.45	0.337	0.014	$\|H \to L; H-1 \to L+2\rangle - c.c.(0.3992)$
					$\|H \to L+8\rangle - c.c.(0.2341)$
	$11^1B^+_{2u}$	5.45	0.351	0.015	$\|H \to L; H-1 \to L+1; H-1 \to L+1\rangle\ (-0.4912)$
					$\|H \to L; H \to L; H-1 \to L+1\rangle\ (-0.2510)$
VIII	$7^1B^+_{3u}$	5.59	0.584	0.044	$\|H \to L+8\rangle\ (0.3796)$
					$\|H-1 \to L+6\rangle - c.c.(0.2866)$
	$14^1B^+_{2u}$	5.62	0.332	0.014	$\|H \to L+12\rangle + c.c.(0.4160)$
					$\|H-1 \to L+7\rangle + c.c.(0.2309)$
	$15^1B^+_{2u}$	5.63	0.326	0.014	$\|H \to L+9\rangle + c.c.(0.3036)$
					$\|H-1 \to L+7\rangle + c.c.(0.2945)$
IX	$8^1B^+_{3u}$	5.89	0.913	0.113	$\|H-2 \to L+4\rangle - c.c.(0.3596)$
					$\|H-1 \to L+6\rangle - c.c.(0.2949)$
	$17^1B^+_{2u}$	5.89	0.149	0.003	$\|H \to L; H-1 \to L+4\rangle - c.c.(0.4687)$
					$\|H \to L; H \to L; H-2 \to L+2\rangle\ (-0.1847)$

Table 6: Excited states contributing to the singlet linear absorption spectrum of decacene computed using the MRSDCI method coupled with the screened parameters in the PPP model Hamiltonian. The rest of the information is same as that in Table 1.

Peak	State	E (eV)	Transition Dipole (Å)	ROS	dominant contributing configurations
DF	$1^1B^-_{3u}$	1.15	0	0	$\|H \rightarrow L; H \rightarrow L+1\rangle - c.c.(0.4851)$
					$\|H \rightarrow L+1; H-1 \rightarrow L+2\rangle - c.c.(0.2102)$
I	$1^1B^+_{2u}$	1.27	1.369	0.067	$\|H \rightarrow L\rangle\ (-0.8338)$
					$\|H \rightarrow L; H \rightarrow L; H-1 \rightarrow L+1\rangle\ (+0.1112)$
II	$2^1B^+_{2u}$	2.16	0.929	0.052	$\|H-1 \rightarrow L+1\rangle\ (+0.7110)$
					$\|H \rightarrow L+2\rangle + c.c.(0.2625)$
III	$3^1B^+_{2u}$	2.42	0.417	0.012	$\|H \rightarrow L+2\rangle + c.c.(0.5220)$
					$\|H-1 \rightarrow L+1\rangle\ (-0.3185)$
	$1^1B^+_{3u}$	2.42	0.295	0.006	$\|H \rightarrow L; H \rightarrow L+1\rangle + c.c.(0.4762)$
					$\|H-1 \rightarrow L; H-1 \rightarrow L+1\rangle + c.c.(0.2590)$
IV	$2^1B^+_{3u}$	3.20	1.872	0.315	$\|H \rightarrow L+1; H \rightarrow L+2\rangle + c.c.(0.3455)$
					$\|H \rightarrow L+5\rangle + c.c.(0.2733)$
	$4^1B^+_{2u}$	3.21	0.706	0.045	$\|H-2 \rightarrow L+2\rangle\ (0.5140)$
					$\|H-1 \rightarrow L+3\rangle + c.c.(0.3975)$
V	$4^1B^+_{3u}$	3.35	3.259	1.000	$\|H \rightarrow L+5\rangle + c.c.(0.4970)$
					$\|H \rightarrow L; H-1 \rightarrow L+2\rangle - c.c.(0.2002)$
VI	$6^1B^+_{3u}$	3.81	0.273	0.008	$\|H \rightarrow L; H \rightarrow L+1\rangle - c.c.(0.3703)$
					$\|H \rightarrow L; H \rightarrow L+3\rangle + c.c.(0.3689)$
VII	$8^1B^+_{3u}$	4.32	0.184	0.004	$\|H \rightarrow L; H-1 \rightarrow L+4\rangle - c.c.(0.2891)$
					$\|H \rightarrow L+6; H-5 \rightarrow L+2\rangle - c.c.(0.2750)$
	$10^1B^+_{2u}$	4.33	0.478	0.028	$\|H-1 \rightarrow L+7\rangle - c.c.(0.2951)$
					$\|H-2 \rightarrow L+4\rangle - c.c.(0.2793)$
VIII	$9^1B^+_{3u}$	4.51	0.330	0.014	$\|H \rightarrow L+8\rangle + c.c.(0.4467)$
					$\|H \rightarrow L+2; H-1 \rightarrow L+2\rangle + c.c.(0.2155)$
	$14^1B^+_{2u}$	4.56	0.376	0.018	$\|H \rightarrow L+9\rangle + c.c.(0.4944)$
					$\|H-3 \rightarrow L+7\rangle\ (-0.2478)$
IX	$11^1B^+_{3u}$	4.77	0.754	0.076	$\|H-2 \rightarrow L+5\rangle + c.c.(0.5543)$
					$\|H \rightarrow L+3; H-1 \rightarrow L+1\rangle - c.c.(0.2076)$
	$16^1B^+_{2u}$	4.77	0.520	0.036	$\|H-1 \rightarrow L+7\rangle - c.c.(0.3795)$
					$\|H-3 \rightarrow L+7\rangle\ (0.3359)$

Triplet absorption

In the following, we discuss in detail the calculated triplet absorption spectra of octacene, nonacene, and decacene, presented in Figures 8–10 of the main text for the standard and the screened parameters. Furthermore, Tables 7–12, provide exhaustive information about the excited states contributing to the triplet spectra of these oligomers.

1. The first peak always corresponds to the $1^3B_{1g}^-$ excited state of the system, whose wave function is dominated by the single excitations $|H \rightarrow L+1\rangle + c.c.$, irrespective of the oligoacene in question, or the Coulomb parameters employed.

2. The second peak corresponds to a y-polarized transition to the $1^3A_g^-$ excited state, for all the oligoacenes, irrespective of the Coulomb parameters employed. The most important configuration contributing to the many-particle wave function of the $1^3A_g^-$ state, is the double excitation $|H \rightarrow L;\, H-1 \rightarrow L+1\rangle$.

3. The nature of the third peak is dependent upon the Coulomb parameters employed in the PPP model. For the standard parameter case, this peak corresponds to a mixture of x- and y-polarized the transitions to states, $2^3B_{1g}^-$ and $3^3A_g^-$ for octacene and nonacene. For octacene, the single excitations $|H \rightarrow L+4\rangle + c.c.$ for the $2^3B_{1g}^-$ state, and $|H-1 \rightarrow L+3\rangle + c.c.$ for $3^3A_g^-$ state contribute the most to the respective wave functions. For nonacene, the single excitations $|H \rightarrow L+3\rangle + c.c.$ for the $2^3B_{1g}^-$ state, and the double excitation $|H \rightarrow L;\, H-1 \rightarrow L+1\rangle$ for the $3^3A_g^-$ states dominate the corresponding wave functions. However, for decacene, the peak corresponds to an x polarized transition to the state $2^3B_{1g}^-$, whose wave function is dominated by single excitations, with the configurations $|H \rightarrow L+3\rangle + c.c.$ contributing the most.

   For the screened parameter case, for all the oligomers, the third peak is due to an x-polarized transition to the state $3^3B_{1g}^-$ whose wave function derives the maximum contribution from the single excitations $|H \rightarrow L+3\rangle + c.c.$.

4. As far as the fourth peak is concerned, with standard parameters it corresponds to an x-polarized transition to the $3^3B_{1g}^-$ excited state, for all the oligoacenes. For octacene, it happens to be the most intense peak of the spectrum, but for nonacene and decacene, it is a shoulder to the most intense peak. Double excitations $|H \rightarrow L;\ H \rightarrow L+3\rangle + c.c.$ contribute the most to the many-particle wave function of this state for octacene, whereas for nonacene and decacene, the single excitations $|H-1 \rightarrow L+2\rangle + c.c.$ dominate the wave function.

   In the screened parameter spectrum, the fourth peak is due to a y-polarized transiton to the $3^3A_g^-$ state for octacene and nonacene. For octacene, the single excitations $|H \rightarrow L+5\rangle + c.c.$ contribute the most to the many particle wave function of this state, while for nonacene, the single excitations $|H \rightarrow L+6\rangle + c.c.$ dominate the state. However, for decacene, the fourth peak is the second most intense peak of the spectrum, corresponding to an x-polarized transition to the $6^3B_{1g}^-$ state, whose wave function is dominated by the double excitations $|H \rightarrow L;\ H \rightarrow L+5\rangle + c.c.$.

5. For the standard parameter case, the fifth peak is due to an x-polarized transition to the state $4^3B_{1g}^-$ for all the oligoacenes. For the case of octacene, it appears as a shoulder of the most intense peak (peak IV), while for nonacene and decacene it is the most intense peak. For octacene the wave function of this state is composed mainly of single excitations, with configurations $|H-1 \rightarrow L+2\rangle + c.c.$ contributing the most. For nonacene and decacene, however, the wave function is dominated by the double excitations $|H \rightarrow L;\ H \rightarrow L+4\rangle + c.c.$.

   In the screened parameter spectrum also the fifth peak corresponds to an x polarized transition for all the oligomers. For octacene, nonacene, and decacene, the states involved are $4^3B_{1g}^-$, $6^3B_{1g}^-$, and $8^3B_{1g}^-$, respectively. For octacene and nonacene, this peak is the second most intense one of the corresponding spectra, and the most im-

portant configuration contributing to the many-particle wave function of the states are the double excitations $|H \rightarrow L;\, H \rightarrow L+4\rangle + c.c.$. However, for decacene, it is a relatively weaker feature, with the double excitations $|H-1 \rightarrow L;\, H \rightarrow L+6\rangle + c.c.$ dominating the wave function of the state.

6. The sixth peak in the standard parameter spectrum, is formed by a y-polarized transition to the state $9^3A_g^-$ for the case of octacene, whose wave function is dominated by the single excitations $|H \rightarrow L+5\rangle + c.c.$ and $|H-3 \rightarrow L+1\rangle + c.c.$ However, for nonacene and decacene, it corresponds to an x-polarized transition to the state $6^3B_{1g}^-$, whose wave function receives maximum contribution from the triple excitations $|H \rightarrow L+1;\, H \rightarrow L+1;\, H-1 \rightarrow L\rangle + c.c.$.

   With the screened parameters, this peak is formed by an x-polarized transition to the state $7^3B_{1g}^-$ for octacene, with double excitations $|H \rightarrow L+1;\, H-5 \rightarrow L\rangle + c.c.$ dominating its wave function. For nonacene and decacene, the peak is due to mixed x and y polarized transitions. For nonacene, states $8^3B_{1g}^-$ and $10^3A_g^-$ form this peak, with their wave functions dominated by double excitations $|H \rightarrow L+1;\, H-6 \rightarrow L+1\rangle + c.c.$, and $|H-1 \rightarrow L+1;\, H \rightarrow L+2\rangle + c.c.$, respectively. For decacene, the states involved are $11^3B_{1g}^-$ and $14^3A_g^-$, with their wave functions dominated by the double excitations $|H \rightarrow L+1;\, H-1 \rightarrow L+5\rangle + c.c.$, and single excitations $|H-1 \rightarrow L+8\rangle + c.c.$, respectively.

7. With the the standard parameters, peak VII for octacene corrresponds to an x-polarized transition to the state $7^3B_{1g}^-$ with the double excitations $|H \rightarrow L;\, H-2 \rightarrow L+3\rangle + c.c.$ dominating its wave function. However, for nonacene and decacene this peak corresponds to a mixed x- and y-polarized transition. For nonacene, the states involved are $7^3B_{1g}^-$ and $11^3A_g^-$, with the double excitations $|H \rightarrow L+1;\, H-5 \rightarrow L\rangle + c.c.$, and single excitations $|H \rightarrow L+5\rangle + c.c.$, contributing the most to their respective wave

functions. For decacene, the states forming the peak are $8^3B_{1g}^-$ and $11^3A_g^-$, of which the former is dominated by the double and triple excitations, while the latter consists mainly of the single excitations.

Screened parameter calculations predict peak VII to have a mixed x and y polarized character for all the oligomers. For the case of octacene, four states $11^3B_{1g}^-$, $12^3B_{1g}^-$, $11^3A_g^-$, and $12^3A_g^-$, form this peak and the double excitations dominate the wave function of the first three states, while $12^3A_g^-$ is dominated by the single excitations. For nonacene, two states $11^3B_{1g}^-$ and $12^3A_g^-$ shape the peak with the triple excitations ($|H \rightarrow L;\, H \rightarrow L;\, H-1 \rightarrow L+2\rangle + c.c.$) dominating the wave function of the former, and single excitations ($|H-1 \rightarrow L+8\rangle + c.c.$) that of the latter. For decacene, three states, $13^3B_{1g}^-$, $14^3B_{1g}^-$, and $15^3A_g^-$, contribute to the peak, with the double excitations dominating all their wave functions.

8. In the standard parameter spectrum, peak VIII has a mixed x and y polarized character for octacene, but only a y-polarized character for nonacene and decacene. For octacene, the peak is formed by states $8^3B_{1g}^-$ and $12^3A_g^-$, of which the wave function of the former is dominated by the triple and double excitations, while that of the latter by double and single excitations. For nonacene, the state in question is $13^3A_g^-$, while for decacene it is $12^3A_g^-$, and wave functions in both the cases are dominated by doubly-excited configurations.

   In the screened parameter calculations, peak VIII exists only for octacene and nonacene, and is due to an x-polarized transition. For octacene it is formed by the state $13^3B_{1g}^-$, whose wave function is dominated by both single and double excitations. For nonacene, the peak is caused by the state $12^3B_{1g}^-$, whose wave function mainly consists of double excitations.

Table 7: Excited states contributing to the triplet absorption spectrum of octacene computed using the MRSDCI method coupled with the standard parameters in the PPP model Hamiltonian. The table includes many-particle dominant contributing configurations, excitation energies, dipole matrix elements, and relative oscillator strengths (ROS) of various states. The excitation energies are with respect to the $1^1A_g^-$, ground state, while the dipole matrix elements, and the ROS, are with respect to the $1^3B_{2u}^+$ state. Below, '$+c.c.$' indicates that the coefficient of charge conjugate of a given configuration has the same sign, while '$-c.c.$' implies that the two coefficients have opposite signs.

Peak	State	E (eV)	Transition Dipole (Å)	ROS	dominant contributing configurations
I	$1^3B_{1g}^-$	3.04	2.950	0.839	$\|H \rightarrow L+1\rangle - c.c.(0.5638)$
					$\|H-1 \rightarrow L+2\rangle + c.c.(0.1836)$
II	$1^3A_g^-$	3.89	0.997	0.123	$\|H \rightarrow L; H-1 \rightarrow L+1\rangle$ (0.8187)
					$\|H \rightarrow L; H-2 \rightarrow L+2\rangle$ (0.1135)
III	$3^3A_g^-$	4.28	0.355	0.017	$\|H-1 \rightarrow L+3\rangle - c.c.(0.3698)$
					$\|H \rightarrow L+5\rangle - c.c.(0.3435)$
	$2^3B_{1g}^-$	4.35	0.579	0.046	$\|H \rightarrow L+4\rangle - c.c.(0.5362)$
					$\|H-1 \rightarrow L+2\rangle + c.c.(0.1999)$
IV	$3^3B_{1g}^-$	5.06	2.494	1.000	$\|H \rightarrow L; H \rightarrow L+3\rangle - c.c.(0.4566)$
					$\|H-1 \rightarrow L+2\rangle + c.c.(0.3011)$
V	$4^3B_{1g}^-$	5.26	1.199	0.240	$\|H-1 \rightarrow L+2\rangle + c.c.(0.3688)$
					$\|H \rightarrow L; H \rightarrow L+3\rangle - c.c.(0.2757)$
VI	$9^3A_g^-$	5.82	0.588	0.064	$\|H \rightarrow L+5\rangle - c.c.(0.3967)$
					$\|H-3 \rightarrow L+1\rangle - c.c.(0.3809)$
VII	$7^3B_{1g}^-$	6.10	1.055	0.216	$\|H \rightarrow L; H-2 \rightarrow L+3\rangle - c.c.(0.4326)$
					$\|H \rightarrow L+1; H-1 \rightarrow L+3\rangle - c.c.(0.1274)$
VIII	$8^3B_{1g}^-$	6.29	0.864	0.149	$\|H \rightarrow L+1; H \rightarrow L+1; H-1 \rightarrow L\rangle - c.c.(0.4030)$
					$\|H \rightarrow L; H-2 \rightarrow L+3\rangle - c.c.(0.3504)$
	$12^3A_g^-$	6.29	0.149	0.004	$\|H-1 \rightarrow L+1; H \rightarrow L+2\rangle - c.c.(0.3707)$
					$\|H-3 \rightarrow L+4\rangle - c.c.(0.2968)$

Table 8: Excited states contributing to the triplet absorption spectrum of octacene computed using the MRSDCI method coupled with the screened parameters in the PPP model Hamiltonian. The rest of the information is same as that in Table 7.

Peak	State	E (eV)	Transition Dipole (Å)	ROS	dominant contributing configurations
I	$1^3B_{1g}^-$	1.97	4.639	1.000	$\|H \rightarrow L+1\rangle + c.c.(0.5936)$
					$\|H-1 \rightarrow L+2\rangle + c.c.(0.0990)$
II	$1^3A_g^-$	2.92	0.996	0.064	$\|H \rightarrow L; H-1 \rightarrow L+1\rangle$ (0.8333)
					$\|H-1 \rightarrow L; H-1 \rightarrow L+2\rangle - c.c.(0.1090)$
III	$3^3B_{1g}^-$	3.39	0.465	0.017	$\|H \rightarrow L+3\rangle + c.c.(0.4280)$
					$\|H-1 \rightarrow L+2\rangle + c.c.(0.3614)$
IV	$3^3A_g^-$	3.68	0.621	0.034	$\|H \rightarrow L+5\rangle + c.c.(0.4915)$
					$\|H-1 \rightarrow L+4\rangle + c.c.(0.3220)$
V	$4^3B_{1g}^-$	4.01	2.601	0.641	$\|H \rightarrow L; H \rightarrow L+4\rangle - c.c.(0.5605)$
					$\|H \rightarrow L+1; H-1 \rightarrow L+4\rangle - c.c.(0.1764)$
VI	$7^3B_{1g}^-$	4.67	1.017	0.114	$\|H \rightarrow L+1; H-5 \rightarrow L\rangle - c.c.(0.5190)$
					$\|H \rightarrow L+1; H-1 \rightarrow L+4\rangle - c.c.(0.2712)$
VII	$11^3A_g^-$	5.13	0.151	0.003	$\|H-1 \rightarrow L+1; H \rightarrow L+2\rangle - c.c.(0.3311)$
					$\|H-1 \rightarrow L+8\rangle - c.c.(0.2700)$
	$11^3B_{1g}^-$	5.15	0.768	0.072	$\|H \rightarrow L+1; H-1 \rightarrow L+4\rangle - c.c.(0.4913)$
					$\|H \rightarrow L+1; H-5 \rightarrow L\rangle - c.c.(0.2874)$
	$12^3B_{1g}^-$	5.18	0.345	0.015	$\|H \rightarrow L+1; H-5 \rightarrow L\rangle - c.c.(0.4987)$
					$\|H \rightarrow L+1; H-1 \rightarrow L+4\rangle - c.c.(0.2693)$
	$12^3A_g^-$	5.19	0.148	0.003	$\|H-1 \rightarrow L+8\rangle + c.c.(0.3959)$
					$\|H \rightarrow L; H-1 \rightarrow L+3\rangle - c.c.(0.2687)$
VIII	$13^3B_{1g}^-$	5.39	0.777	0.077	$\|H-1 \rightarrow L+8\rangle + c.c.(0.3959)$
					$\|H \rightarrow L; H-1 \rightarrow L+3\rangle - c.c.(0.2687)$

Table 9: Excited states contributing to the triplet absorption spectrum of nonacene computed using the MRSDCI method coupled with the standard parameters in the PPP model Hamiltonian. The rest of the information is same as that in Table 7.

Peak	State	E (eV)	Transition Dipole (Å)	ROS	dominant contributing configurations
I	$1^3B_{1g}^-$	2.56	3.331	0.785	$\|H \rightarrow L+1\rangle + c.c.(0.5522)$
					$\|H-1 \rightarrow L+2\rangle + c.c.(0.1825)$
II	$1^3A_g^-$	3.30	1.018	0.095	$\|H \rightarrow L; H-1 \rightarrow L+1\rangle$ (0.8148)
					$\|H \rightarrow L; H-1 \rightarrow L+3\rangle$ $c.c.(0.1109)$
III	$2^3B_{1g}^-$	3.79	0.686	0.049	$\|H \rightarrow L+3\rangle - c.c.(0.5156)$
					$\|H-1 \rightarrow L+2\rangle + c.c.(0.2173)$
	$3^3A_g^-$	3.89	0.352	0.013	$\|H \rightarrow L; H-1 \rightarrow L+1\rangle$ (0.4041)
					$\|H-1 \rightarrow L+4\rangle - c.c.(0.3279)$
IV	$3^3B_{1g}^-$	4.39	0.790	0.076	$\|H-1 \rightarrow L+2\rangle + c.c.(0.4226)$
					$\|H \rightarrow L; H \rightarrow L; H-1 \rightarrow L+2\rangle + c.c.(0.2222)$
V	$4^3B_{1g}^-$	4.66	2.789	1.000	$\|H \rightarrow L; H \rightarrow L+4\rangle + c.c.(0.5047)$
					$\|H-1 \rightarrow L; H \rightarrow L+5\rangle - c.c.(0.2034)$
VI	$6^3B_{1g}^-$	5.14	0.418	0.025	$\|H \rightarrow L+1; H \rightarrow L+1; H-1 \rightarrow L\rangle + c.c.(0.4111)$
					$\|H \rightarrow L; H \rightarrow L+4\rangle + c.c.(0.2905)$
VII	$11^3A_g^-$	5.39	0.517	0.040	$\|H \rightarrow L+5\rangle - c.c.(0.3654)$
					$\|H-1 \rightarrow L+4\rangle - c.c.(0.3219)$
	$7^3B_{1g}^-$	5.44	1.438	0.310	$\|H \rightarrow L+1; H-5 \rightarrow L\rangle - c.c.(0.4435)$
					$\|H \rightarrow L+1; H \rightarrow L+4\rangle - c.c.(0.3271)$
VIII	$13^3A_g^-$	5.75	0.428	0.029	$\|H-1 \rightarrow L+1; H \rightarrow L+2\rangle - c.c.(0.2992)$
					$\|H \rightarrow L; H-1 \rightarrow L+3\rangle - c.c.(0.2305)$

Table 10: Excited states contributing to the triplet absorption spectrum of nonacene computed using the MRSDCI method coupled with the screened parameters in the PPP model Hamiltonian. The rest of the information is same as that in Table 7.

Peak	State	E (eV)	Transition Dipole (Å)	ROS	dominant contributing configurations
I	$1^3B_{1g}^-$	1.86	5.218	1.000	$\|H \rightarrow L+1\rangle + c.c.(0.5919)$
					$\|H-1 \rightarrow L+2\rangle - c.c.(0.1143)$
II	$1^3A_g^-$	2.61	1.032	0.055	$\|H \rightarrow L; H-1 \rightarrow L+1\rangle$ (0.8266)
					$\|H-1 \rightarrow L; H \rightarrow L+2\rangle + c.c.(0.1122)$
III	$3^3B_{1g}^-$	3.14	0.711	0.031	$\|H \rightarrow L+3\rangle + c.c.(0.4278)$
					$\|H-1 \rightarrow L+2\rangle - c.c.(0.3551)$
IV	$3^3A_g^-$	3.58	0.514	0.019	$\|H \rightarrow L+6\rangle + c.c.(0.4657)$
					$\|H-1 \rightarrow L+4\rangle - c.c.(0.3453)$
V	$6^3B_{1g}^-$	4.09	2.577	0.535	$\|H \rightarrow L; H \rightarrow L+4\rangle + c.c.(0.5088)$
					$\|H-1 \rightarrow L; H \rightarrow L+1; H \rightarrow L+1\rangle + c.c.(0.2302)$
VI	$10^3A_g^-$	4.52	0.324	0.009	$\|H-1 \rightarrow L+1; H \rightarrow L+2\rangle - c.c.(0.3581)$
					$\|H \rightarrow L; H-1 \rightarrow L+3\rangle - c.c.(0.2788)$
	$8^3B_{1g}^-$	4.53	1.434	0.184	$\|H \rightarrow L+1; H-6 \rightarrow L+1\rangle - c.c.(0.5621)$
					$\|H-2 \rightarrow L+3\rangle - c.c.(0.1869)$
VII	$11^3B_{1g}^-$	4.87	0.398	0.015	$\|H \rightarrow L; H \rightarrow L; H-1 \rightarrow L+2\rangle - c.c.(0.4361)$
					$\|H-1 \rightarrow L; H-1 \rightarrow L; H \rightarrow L+1\rangle + c.c.(0.3273)$
	$12^3A_g^-$	4.92	0.215	0.004	$\|H-1 \rightarrow L+8\rangle + c.c.(0.4643)$
					$\|H \rightarrow L; H-1 \rightarrow L+3\rangle - c.c.(0.2204)$
VIII	$12^3B_{1g}^-$	5.14	0.884	0.079	$\|H \rightarrow L+1; H-6 \rightarrow L+1\rangle - c.c.(0.5873)$
					$\|H \rightarrow L; H-1 \rightarrow L+2\rangle - c.c.(0.0756)$

Table 11: Excited states contributing to the triplet absorption spectrum of decacene computed using the MRSDCI method coupled with the standard parameters in the PPP model Hamiltonian. The rest of the information is same as that in Table 7.

Peak	State	E (eV)	Transition Dipole (Å)	ROS	dominant contributing configurations
I	$1^3B_{1g}^-$	2.49	3.615	1.000	$\|H \rightarrow L+1\rangle - c.c.(0.5461)$
					$\|H-1 \rightarrow L+2\rangle + c.c.(0.1918)$
II	$1^3A_g^-$	3.16	1.097	0.117	$\|H \rightarrow L; H-1 \rightarrow L+1\rangle$ (0.8189)
					$\|H \rightarrow L; H-1 \rightarrow L+3\rangle - c.c.(0.1177)$
III	$2^3B_{1g}^-$	3.62	0.800	0.071	$\|H \rightarrow L+3\rangle - c.c.(0.5228)$
					$\|H-1 \rightarrow L+2\rangle + c.c.(0.1965)$
IV	$3^3B_{1g}^-$	4.35	0.793	0.084	$\|H-1 \rightarrow L+2\rangle + c.c.(0.4745)$
					$\|H-1 \rightarrow L+4\rangle - c.c.(0.1760)$
V	$4^3B_{1g}^-$	4.62	2.534	0.912	$\|H \rightarrow L; H \rightarrow L+4\rangle - c.c.(0.4009)$
					$\|H \rightarrow L+7\rangle - c.c.(0.2788)$
VI	$6^3B_{1g}^-$	5.22	1.183	0.225	$\|H \rightarrow L+1; H \rightarrow L+1; H-1 \rightarrow L\rangle - c.c.(0.3604)$
					$\|H \rightarrow L+1; H-6 \rightarrow L\rangle - c.c.(0.3314)$
VII	$11^3A_g^-$	5.42	0.493	0.040	$\|H \rightarrow L+6\rangle + c.c.(0.3537)$
					$\|H-1 \rightarrow L+4\rangle - c.c.(0.3086)$
	$8^3B_{1g}^-$	5.44	1.179	0.232	$\|H \rightarrow L+1; H-1 \rightarrow L; H-1 \rightarrow L\rangle - c.c.(0.3928)$
					$\|H \rightarrow L+1; H-6 \rightarrow L\rangle - c.c.(0.3365)$
VIII	$12^3A_g^-$	5.70	0.456	0.036	$\|H-1 \rightarrow L+1; H \rightarrow L+2\rangle - c.c.(0.3473)$
					$\|H \rightarrow L+1; H \rightarrow L+3\rangle - c.c.(0.2317)$

Table 12: Excited states contributing to the triplet absorption spectrum of decacene computed using the MRSDCI method coupled with the screened parameters in the PPP model Hamiltonian. The rest of the information is same as that in Table 7.

Peak	State	E (eV)	Transition Dipole (Å)	ROS	dominant contributing configurations
I	$1^3B_{1g}^-$	1.72	5.841	1.000	$\|H \rightarrow L+1\rangle - c.c.(0.5872)$
					$\|H-1 \rightarrow L+2\rangle - c.c.(0.1112)$
II	$1^3A_g^-$	2.33	1.074	0.046	$\|H \rightarrow L; H-1 \rightarrow L+1\rangle\ (0.8198)$
					$\|H \rightarrow L; H-1 \rightarrow L+2\rangle - c.c.(0.0986)$
III	$3^3B_{1g}^-$	2.89	0.831	0.034	$\|H \rightarrow L+3\rangle - c.c.(0.4352)$
					$\|H-1 \rightarrow L+2\rangle - c.c.(0.3443)$
IV	$6^3B_{1g}^-$	3.80	2.695	0.470	$\|H \rightarrow L; H \rightarrow L+5\rangle - c.c.(0.5362)$
					$\|H \rightarrow L+1; H-1 \rightarrow L+5\rangle - c.c.(0.1922)$
V	$8^3B_{1g}^-$	4.24	1.266	0.116	$\|H-1 \rightarrow L; H \rightarrow L+6\rangle - c.c.(0.4998)$
					$\|H \rightarrow L+1; H-1 \rightarrow L+5\rangle - c.c.(0.3005)$
VI	$11^3B_{1g}^-$	4.70	0.791	0.050	$\|H \rightarrow L+1; H-1 \rightarrow L+5\rangle - c.c.(0.4721)$
					$\|H \rightarrow L+1; H-6 \rightarrow L\rangle - c.c.(0.3044)$
	$14^3A_g^-$	4.72	0.135	0.001	$\|H-1 \rightarrow L+8\rangle - c.c.(0.4705)$
					$\|H-3 \rightarrow L+5\rangle - c.c.(0.2190)$
VII	$13^3B_{1g}^-$	4.90	1.001	0.084	$\|H \rightarrow L+1; H-5 \rightarrow L+1\rangle - c.c.(0.3314)$
					$\|H \rightarrow L+13\rangle - c.c.(0.3095)$
	$14^3B_{1g}^-$	4.91	0.638	0.034	$\|H \rightarrow L+13\rangle - c.c.(0.4517)$
					$\|H \rightarrow L+1; H-5 \rightarrow L+1\rangle - c.c.(0.2219)$
	$15^3A_g^-$	4.91	0.162	0.002	$\|H-1 \rightarrow L+1; H \rightarrow L+4\rangle - c.c.(0.4666)$
					$\|H-1 \rightarrow L+1; H-2 \rightarrow L+2\rangle\ (0.4449)$

References

(1) Raghu, C.; Pati, Y. A.; Ramasesha, S. Structural and Electronic Instabilities in Polyacenes: Density-Matrix Renormalization Group Study of a Long-Range Interacting Model. *Phys. Rev. B* **2002**, *65*, 155204.

(2) Raghu, C.; Anusooya Pati, Y.; Ramasesha, S. Density-Matrix Renormalization-Group Study of Low-Lying Excitations of Polyacene within a Pariser-Parr-Pople Model. *Phys. Rev. B* **2002**, *66*, 035116.

(3) Bendikov, M.; Duong, H. M.; Starkey, K.; Houk, K. N.; Carter, E. A.; Wudl, F. Oligoacenes: Theoretical Prediction of Open-Shell Singlet Diradical Ground States. *J. Am. Chem. Soc.* **2004**, *126*, 7416–7417.

(4) Hachmann, J.; Dorando, J. J.; Aviles, M.; Chan, G. K.-L. The Radical Character of the Acenes: A Density Matrix Renormalization Group Study. *J. Chem. Phys.* **2007**, *127*, 134309.

(5) Hajgató, B.; Huzak, M.; Deleuze, M. S. Focal Point Analysis of the Singlet-Triplet Energy Gap of Octacene and Larger Acenes. *J. Phys. Chem. A* **2011**, *115*, 9282–9293.

(6) Sony, P.; Shukla, A. Large-Scale Correlated Calculations of Linear Optical Absorption and Low-Lying Excited States of Polyacenes: Pariser-Parr-Pople Hamiltonian. *Phys. Rev. B* **2007**, *75*, 155208.

(7) Sony, P.; Shukla, A. Large-Scale Correlated Study of Excited State Absorptions in Naphthalene and Anthracene. *J. Chem. Phys.* **2009**, *131*, 014302.